Available online at www.sciencedirect.com
ScienceDirect
Mendeleev Commun., 2020, **30**, 476–478

Mendeleev Communications

Four-component relativistic computational NMR study of ferrous, cobalt and nickel bisglycinates

Valentin A. Semenov, Dmitry O. Samultsev and Leonid B. Krivdin*

A. E. Favorsky Irkutsk Institute of Chemistry, Siberian Branch of the Russian Academy of Sciences, 664033 Irkutsk, Russian Federation. E-mail: krivdin_office@irioch.irk.ru

DOI: 10.1016/j.mencom.2020.07.023

The equilibrium structures of ferrous(II), cobalt(III) and nickel(II) bisglycinates were optimized at the DFT level using eight functionals, and their ^{1}H, ^{13}C, ^{15}N and ^{17}O NMR chemical shifts were evaluated at both non-relativistic and four-component relativistic levels. Essential deshielding relativistic corrections were observed for nitrogen and oxygen, while they were found to be small for carbons and protons. Solvent corrections for chemical shifts noticeably increased with the dielectric constant of a solvent for nitrogen and carbon, and they were negligibly small for protons.

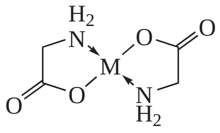

M = Fe, Co, Ni

Keywords: relativistic effects, ferrous, cobalt and nickel bisglycinates, NMR chemical shifts, DFT.

Transition metal complexes play an important role in the modern pharmaceutical industry as anticancer, antiviral and antibacterial drugs because they participate in various biological processes, including synthesis, acid–base catalysis, and redox processes. Metal complexes with organic ligands are simplified structural analogues of metal enzymes since their metal ions are usually coordinated by nitrogen, oxygen or sulfur donor groups similarly to peptide residues. For example, the simplest amino acid glycine can form chelate complexes with manganese, cobalt, nickel, iron, zinc, *etc.*,[1] and some glycine transition metal complexes are widely used as food additives.[2]

In continuation of our studies on computational NMR of transition metal complexes such as cisplatin, transplatin[3] and their derivatives,[4] we report here the results of a four-component relativistic DFT study of ^{1}H, ^{13}C, ^{15}N and ^{17}O NMR chemical shifts of ferrous, cobalt and nickel bisglycinates **1**–**3**.

The fundamentals of computational NMR were discussed in an encyclopedia by Sauer and in general reviews.[6–11] Specialized reviews concentrated on the practical computation of particular NMR parameters, such as those of proton,[12–14] carbon[15–17] and nitrogen[18] NMR spectra, in line with the results of this work. In addition to the computational NMR of light nuclei, recent advances of a relativistic approach used to calculate the NMR properties of heavier nuclei at relativistic two- and four-component levels were considered.[19–24] Of special interest are the relativistic effects on light nuclei like nitrogen and oxygen provided by neighbouring transition metals like iron, cobalt, and nickel. In this communication, we demonstrate the potential of a fully relativistic four-component Dirac's approach to the structural investigation of ferrous, cobalt and nickel bisglycinates including the calculation of their ^{1}H, ^{13}C, ^{15}N and ^{17}O NMR chemical shifts depending on the central complexing metal.

Geometry optimization of **1**–**3** was performed using the following hybrid exchange–correlation and generalized gradient approximation functionals: B3LYP, the most common three-parameter hybrid functional of Becke[25] in combination with the correlation functional of Lee, Yang and Parr;[26] B3PW91, three-parameter hybrid functional of Becke[25] in combination with the non-local correlation provided by Perdew and Wang;[27] BHandH, Becke's half and half mixing (50 : 50) of a Hartree–Fock exchange and local spin density exchange[28] plus Lee, Yang, and Parr correlation; OLYP, Handy and FCohen's hybrid functional[29] in combination with Lee, Yang, and Parr's correlation functional;[26] O3LYP, a three-parameter Handy and Cohen's hybrid functional[30] in combination with Lee, Yang, and Parr's correlation functional;[26] PBE, the generalized gradient functional of Perdew, Burke, and Ernzerhof;[31] PBE0, the generalized gradient functional of Perdew, Burke, and Ernzerhof[31] with a predetermined amount of exact exchange;[32] and M062X, Minnesota global generalized gradient approximation hybrid exchange–correlation functional.[33] These functionals were used in combination with Dunning's aug-cc-pVTZ basis set.[34] Based on our previous results,[3,4] we employed the Keal–Tozer KT2 functional[35] in combination with the relativistic Dyall's dyall.ae3z basis set[36] on metals and Jensen's aug-pcS-2 basis set[37] on the rest of atoms for the calculation of NMR chemical shifts. The geometrical parameters were optimized with the GAUSSIAN 09 code,[38] while the calculations of chemical shifts (relativistic and non-relativistic) were performed with the DIRAC suite of programs.[39]

Figure 1 shows the optimized structures and salient geometrical parameters of **1**–**3**. The three complexes provide very similar geometries differing noticeably only in bond lengths involving the central complexing metal. Ferrous bisglycinate **1** possesses the largest central bond lengths, while the N–X–O (X = Fe, Co, Ni) bond angles of about 86° are essentially the same in these complexes. Note that the frameworks of the glycine moiety are essentially planar in the three complexes.

First, we tested the performance of different functionals in the geometrical optimization of title three complexes, as compared to experimental data[40,41] (Figure 2). The Minnesota functional

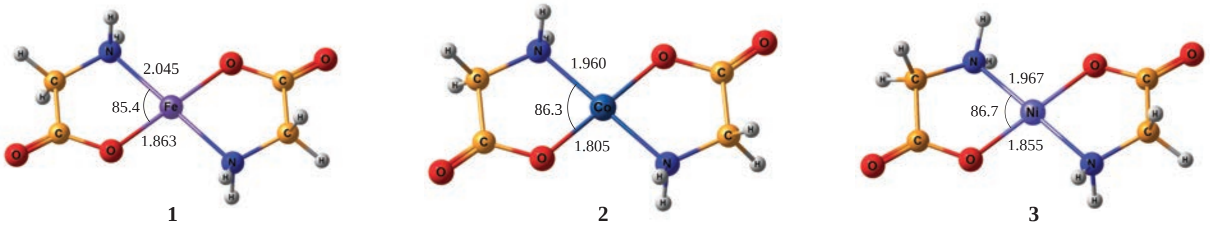

1 **2** **3**

Figure 1 Equilibrium geometries of ferrous, cobalt and nickel bisglycinates **1**–**3** optimized at the M062X/aug-cc-pVTZ level. Bond lengths are given in angstroms, while bond angles are in degrees.

M062X showed the best performance giving a normalized mean absolute error of less than 3% for the $r_{\text{M–N}}$ bond length and about 4% for the $\theta_{\text{N–M–O}}$ bond angle. On the other hand, Becke's half and half functional BHandH demonstrated the largest deviation of 9%. The rest of functionals provided moderate deviations of about 5–7%. Generally, the largest deviations from experimental data were found for M–O (M = Fe, Co, Ni) bond lengths. Based on these results, we used geometrical parameters provided by the Minnesota functional M062X in combination with the aug-cc-pVTZ basis set in the further calculations.

Note that ferrous(II) and nickel(II) bisglycinates are neutral species, while cobalt(III) bisglycinate is a cation; therefore, a charge effect was taken into account at the stage of geometry optimization and in the calculation of NMR chemical shifts. The optimization of the geometric parameters of cobalt bisglycinate **2** as a cation and a neutral complex (aqua bisglycinate with a chlorine anion in the outer sphere) did not reveal significant differences; at least all optimized geometric parameters were within the error range. The same was observed in the calculation of shielding constants (chemical shifts) of **2**: the charge effect was only slightly larger than the mean absolute error of the calculation of NMR chemical shifts. As an example, for the ^{15}N NMR chemical shifts of cobalt bisglycinate, this effect varied from 3 to 5 ppm depending on the basis set.

We analyzed the amount of relativistic correction to the chemical shifts of different light nuclei in **1**–**3** in the neighborhood of the heavy metals (iron, cobalt, and nickel). Table 1 summarizes calculated neat relativistic corrections to ^{1}H, ^{13}C, ^{15}N and ^{17}O NMR chemical shifts of **1**–**3**, and Figure 3 shows the relative ratios of relativistic corrections to chemical shift of the specified nuclei in different chemical environments. The largest deshielding relativistic corrections were observed for nitrogen (10.5, 9.3 and 13.0 ppm induced by iron in **1**, cobalt in **2**, and nickel in **3**, respectively) and oxygen (5–6 ppm), and small corrections were observed for carbon (~1 ppm) and protons (<0.1 ppm). The relative ratios of the relativistic corrections to ^{1}H, ^{13}C, ^{15}N and ^{17}O NMR chemical shifts of **1**–**3** are about 1–3% on average with the only surprising exception for the ^{13}C NMR chemical shift of the (β + γ)-carbonyl group (much less than 1%), as compared to that of the (β + γ)-methylene group (2–3%), which could not be rationalized at this stage.

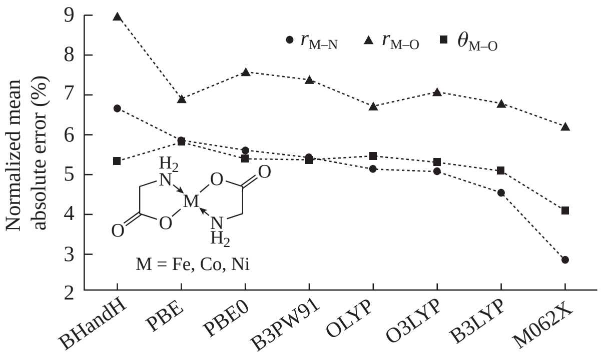

Figure 2 Normalized mean absolute errors of salient geometric parameters in compounds **1**–**3** optimized at the DFT level using different functionals in combination with the aug-cc-pVTZ basis set.

Table 1 NMR chemical shifts of **1**–**3** calculated at the (4c)KT2/dyall.ae3z//aug-pcS-2 level.[a]

Compound	Nuclei	KT2	4c KT2	Relativistic correction
Ferrous bisglycinate **1**	^{1}H (CH$_2$)	2.12	2.16	0.04
	^{1}H (NH$_2$)	3.64	3.55	–0.09
	^{13}C (CH$_2$)	41.8	42.6	0.8
	^{13}C (C=O)	155.2	155.5	0.3
	^{15}N	–353.9	–343.4	10.5
	^{17}O (C–O)	125.1	129.9	4.8
	^{17}O (C=O)	415.7	421.4	5.7
Cobalt bisglycinate **2**	^{1}H (CH$_2$)	1.86	1.88	0.02
	^{1}H (NH$_2$)	1.83	1.92	0.09
	^{13}C (CH$_2$)	38.0	36.8	–1.2
	^{13}C (C=O)	154.9	153.4	–1.5
	^{15}N	–358.7	–349.4	9.3
	^{17}O (C–O)	97.8	99.5	1.7
	^{17}O (C=O)	492.6	489.6	–3.0
Nickel bisglycinate **3**	^{1}H (CH$_2$)	–1.89	–1.82	0.07
	^{1}H (NH$_2$)	1.22	1.28	0.06
	^{13}C (CH$_2$)	39.0	39.9	0.9
	^{13}C (C=O)	155.1	155.5	0.4
	^{15}N	–374.2	–361.2	13.0
	^{17}O (C–O)	200.7	195.1	–5.6
	^{17}O (C=O)	393.0	399.1	6.1

[a] Evaluated as $\delta = \sigma_{st} - \sigma$ (δ is the calculated chemical shift, and σ_{st} and σ are the shielding constants of standard and test compounds, respectively). The calculated NMR chemical shifts are given in ppm with reference to TMS (^{1}H, ^{13}C), nitromethane (^{15}N), and water (^{17}O).

Unfortunately, no experimental data on chemical shifts of **1**–**3** were found in the literature.

Finally, we studied the solvent effect (for dielectric constants ε from 0 to about 180) on calculated ^{1}H, ^{13}C and ^{15}N NMR chemical shifts evaluated within the integral equation formalism polarizable continuum model (IEF–PCM)[42] reviewed by Tomasi *et al.*[43] (Figure 4). It can be seen that absolute solvent corrections to the total chemical shifts increased with dielectric constant (up to 13 ppm for nitrogen and 9 ppm for carbon), and they were negligible for protons (0.1–0.2 ppm). The only exception was observed in

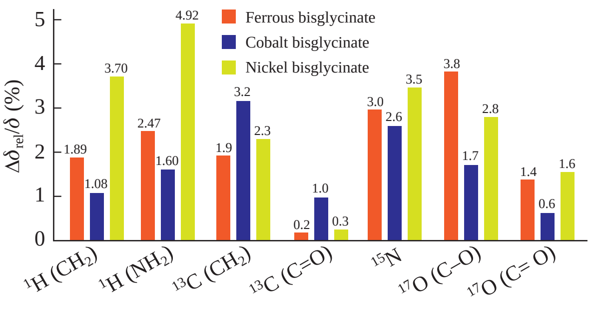

Figure 3 Relative ratios of relativistic corrections to ^{1}H, ^{13}C, ^{15}N and ^{17}O NMR chemical shifts of ferrous, cobalt and nickel bisglycinates.

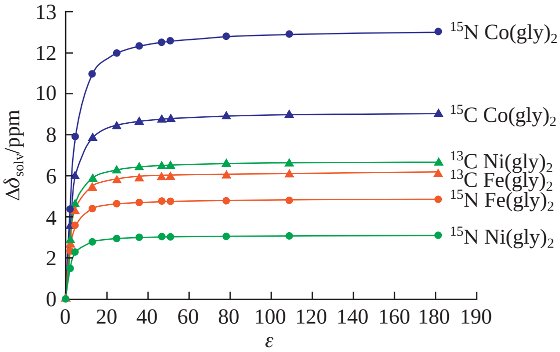

Figure 4 Absolute solvent corrections to calculated ^{13}C and ^{15}N NMR chemical shifts of ferrous, cobalt and nickel bisglycinates.

the ^{1}H NMR chemical shift of the amino group in cobalt bisglycinate **2**. In this case, the average solvent correction was unprecedentedly large (3–5 ppm), as compared to all other protons in this series. This can be due to the fact that complexes **1** and **3** are neutral, while complex **2** is an inner shell of a cationic complex. However, this reasoning requires a special consideration. Full data on solvent corrections to chemical shifts are given in the Online Supplementary Materials.

The general conclusions made in this study are as follows. (i) Ferrous, cobalt, and nickel bisglycinates provide very similar geometries differing noticeably only in bond lengths involving central complexing metals. Ferrous bisglycinate possesses the largest central bond lengths, while the N–X–O (X = Fe, Co, Ni) bond angles of about 86° are essentially the same in all three complexes. The frameworks of the glycine moiety are essentially planar in all three complexes. (ii) The largest deshielding relativistic corrections are observed for nitrogen (10.5 ppm for iron in **1**, 9.3 ppm for cobalt in **2**, and 13.0 ppm for nickel in **3**) and oxygen (5–6 ppm) being small for carbon (~1 ppm) and negligibly small for protons (<0.1 ppm). (iii) Absolute solvent corrections to total chemical shifts increase with dielectric constant (up to 13 ppm for nitrogen and 9 ppm for carbon) being negligibly small for protons (0.1–0.2 ppm).

This work was supported by the Russian Foundation for Basic Research (grant no. 18-33-00334). The calculations were performed at the A. E. Favorsky Irkutsk Institute of Chemistry using the facilities of Baikal Analytical Center and at the Irkutsk Supercomputer Center of the Siberian Branch of the Russian Academy of Sciences using the HPC-cluster ‘Akademik V. M. Matrosov’ (see *http://hpc.icc.ru/en/*, last accessed 24.03.2020). We are grateful to Yu. Rusakov for stimulating discussions and fruitful advices.

Online Supplementary Materials

Supplementary data associated with this article can be found in the online version at doi: 10.1016/j.mencom.2020.07.023.

References

1 G. V. Novikova, A. I. Petrov, N. A. Staloverova, A. S. Samoilov, I. D. Dergachev and A. A. Shubin, *Spectrochim. Acta, Part A*, 2015, **135**, 491.
2 T. E. Fox, J. Eagles and S. J. Fairweather-Tait, *Am. J. Clin. Nutr.*, 1998, **67**, 664.
3 V. A. Semenov, Yu. Yu. Rusakov, D. O. Samultsev and L. B. Krivdin, *Mendeleev Commun.*, 2019, **29**, 315.
4 V. A. Semenov, D. O. Samultsev, I. L. Rusakova and L. B. Krivdin, *J. Phys. Chem. A*, 2019, **123**, 4908.
5 S. P. A. Sauer, *Molecular Electromagnetism: A Computational Chemistry Approach*, Oxford University Press, Oxford, 2011.
6 T. Helgaker, M. Jaszuński and M. Pecul, *Prog. Nucl. Magn. Reson. Spectrosc.*, 2008, **53**, 249.
7 T. Helgaker, S. Coriani, P. Jørgensen, K. Kristensen, J. Olsen and K. Ruud, *Chem. Rev.*, 2012, **112**, 543.
8 G. A. Aucar, R. H. Romero and A. F. Maldonado, *Int. Rev. Phys. Chem.*, 2010, **29**, 1.
9 *High Resolution NMR Spectroscopy: Understanding Molecules and Their Electronic Structures*, ed. R. H. Contreras, Elsevier, Oxford, 2013, vol. 3.
10 Yu. Yu. Rusakov and L. B. Krivdin, *Russ. Chem. Rev.*, 2013, **82**, 99.
11 F. A. A. Mulder and M. Filatov, *Chem. Soc. Rev.*, 2010, **39**, 578.
12 L. B. Krivdin, *Magn. Reson. Chem.*, 2019, **57**, 897.
13 L. B. Krivdin, *Magn. Reson. Chem.*, 2020, **58**, 5.
14 L. B. Krivdin, *Magn. Reson. Chem.*, 2020, **58**, 15.
15 L. B. Krivdin, *Prog. Nucl. Magn. Reson. Spectrosc.*, 2018, **105**, 54.
16 L. B. Krivdin, *Prog. Nucl. Magn. Reson. Spectrosc.*, 2018, **108**, 17.
17 L. B. Krivdin, *Prog. Nucl. Magn. Reson. Spectrosc.*, 2019, **112–113**, 103.
18 L. B. Krivdin, *Prog. Nucl. Magn. Reson. Spectrosc.*, 2017, **102–103**, 98.
19 Y. Xiao, W. Liu and J. Autschbach, in *Handbook of Relativistic Quantum Chemistry*, ed. W. Liu, Springer, Berlin, 2017, pp. 657–692.
20 J. Autschbach, *Philos. Trans. R. Soc. A*, 2014, **372**, 1.
21 J. Autschbach, in *High Resolution NMR Spectroscopy: Understanding Molecules and Their Electronic Structures*, ed. R. H. Contreras, Elsevier, Oxford, 2013, pp. 69–112.
22 M. Repisky, S. Komorovsky, R. Bast and K. Ruud, in *Gas Phase NMR*, eds. K. Jackowski and M. Jaszunski, Royal Society of Chemistry, Cambridge, 2016, pp. 267–303.
23 I. L. Rusakova, Yu. Yu. Rusakov and L. B. Krivdin, *Russ. Chem. Rev.*, 2016, **85**, 356.
24 I. L. Rusakova and L. B. Krivdin, *Mendeleev Commun.*, 2018, **28**, 1.
25 A. D. Becke, *J. Chem. Phys.*, 1993, **98**, 5648.
26 C. Lee, W. Yang and R. G. Parr, *Phys. Rev. B*, 1988, **37**, 785.
27 K. Burke, J. P. Perdew and Y. Wang, in *Electronic Density Functional Theory: Recent Progress and New Directions*, eds. J. F. Dobson, G. Vignale and M. P. Das, Springer, Boston, MA, 1998, pp. 81–111.
28 A. D. Becke, *J. Chem. Phys.*, 1993, **98**, 1372.
29 N. C. Handy and A. J. Cohen, *Mol. Phys.*, 2001, **99**, 403.
30 A. J. Cohen and N. C. Handy, *Mol. Phys.*, 2001, **99**, 607.
31 J. P. Perdew, K. Burke and M. Ernzerhof, *Phys. Rev. Lett.*, 1996, **77**, 3865.
32 C. Adamo and V. Barone, *J. Chem. Phys.*, 1999, **110**, 6158.
33 Y. Zhao and D. G. Truhlar, *Theor. Chem. Acc.*, 2006, **120**, 215.
34 T. H. Dunning, Jr., *J. Chem. Phys.*, 1989, **90**, 1007.
35 T. W. Keal and D. J. Tozer, *J. Chem. Phys.*, 2003, **119**, 3015.
36 K. G. Dyall, *Theor. Chem. Acc.*, 1998, **99**, 366.
37 F. Jensen, *J. Chem. Theory Comput.*, 2008, **4**, 719.
38 M. J. Frisch, G. W. Trucks, H. B. Schlegel, G. E. Scuseria, M. A. Robb, J. R. Cheeseman, G. Scalmani, V. Barone, B. Mennucci, G. A. Petersson, H. Nakatsuji, M. Caricato, X. Li, H. P. Hratchian, A. F. Izmaylov, J. Bloino, G. Zheng, J. L. Sonnenberg, M. Hada, M. Ehara, K. Toyota, R. Fukuda, J. Hasegawa, M. Ishida, T. Nakajima, Y. Honda, O. Kitao, H. Nakai, T. Vreven, J. A. Montgomery, Jr., J. E. Peralta, F. Ogliaro, M. Bearpark, J. J. Heyd, E. Brothers, K. N. Kudin, V. N. Staroverov, R. Kobayashi, J. Normand, K. Raghavachari, A. Rendell, J. C. Burant, S. S. Iyengar, J. Tomasi, M. Cossi, N. Rega, J. M. Millam, M. Klene, J. E. Knox, J. B. Cross, V. Bakken, C. Adamo, J. Jaramillo, R. Gomperts, R. E. Stratmann, O. Yazyev, A. J. Austin, R. Cammi, C. Pomelli, J. W. Ochterski, R. L. Martin, K. Morokuma, V. G. Zakrzewski, G. A. Voth, P. Salvador, J. J. Dannenberg, S. Dapprich, A. D. Daniels, Ö. Farkas, J. B. Foresman, J. V. Ortiz, J. Cioslowski and D. J. Fox, *GAUSSIAN 09, Revision C.01*, Gaussian, Wallingford, CT, 2009. *http://www.gaussian.com*, last visited 2020.
39 H. J. Aa. Jensen, R. Bast, T. Saue and L. Visscher, with contributions from V. Bakken, K. G. Dyall, S. Dubillard, U. Ekstroem, E. Eliav, T. Enevoldsen, E. Fasshauer, T. Fleig, O. Fossgaard, A. S. P. Gomes, T. Helgaker, J. Henriksson, M. Ilias, Ch. R. Jacob, S. Knecht, S. Komorovsky, O. Kullie, J. K. Laerdahl, C. V. Larsen, Y. S. Lee, H. S. Nataraj, M. K. Nayak, P. Norman, G. Olejniczak, J. Olsen, Y. C. Park, J. K. Pedersen, M. Pernpointner, R. Di Remigio, K. Ruud, P. Salek, B. Schimmelpfennig, J. Sikkema, A. J. Thorvaldsen, J. Thyssen, J. van Stralen, S. Villaume, O. Visser, T. Winther and S. Yamamoto, *DIRAC, A Relativistic Ab Initio Electronic Structure Program, Revision DIRAC16*, 2016, *http://www.diracprogram.org*.
40 S. Jungen and P. Chen, *Chem. – Eur. J.*, 2018, **24**, 11008.
41 Z.-L. Wang and Z.-B. Zhang, *Acta Crystallogr.*, 2006, **E62**, m2546.
42 B. Mennucci and J. Tomasi, *J. Chem. Phys.*, 1997, **106**, 5151.
43 J. Tomasi, B. Mennucci and R. Cammi, *Chem. Rev.*, 2005, **105**, 2999.

Received: 28th January 2020; Com. 20/6117